Search for $\Delta S = 2$ Nonleptonic Hyperon Decays

C. G. White,[5],* R. A. Burnstein,[5] A. Chakravorty,[5] A. Chan,[1] Y. C. Chen,[1] W. S. Choong,[2,7] K. Clark,[9] E. C. Dukes,[10]
C. Durandet,[10] J. Felix,[4] G. Gidal,[7] P. Gu,[7] H. R. Gustafson,[8] C. Ho,[1] T. Holmstrom,[10] M. Huang,[10] C. James,[3]
C. M. Jenkins,[9] D. M. Kaplan,[5] L. M. Lederman,[5] N. Leros,[6] M. J. Longo,[8] F. Lopez,[8] L. C. Lu,[10] W. Luebke,[5] K. B. Luk,[2,7]
K. S. Nelson,[10] H. K. Park,[8] J.-P. Perroud,[6] D. Rajaram,[5] H. A. Rubin,[5] P. K. Teng,[1] J. Volk,[3] S. L. White,[5] and P. Zyla[7]

(HyperCP Collaboration)

[1]*Institute of Physics, Academica Sinica, Taipei 11529, Taiwan, Republic of China*
[2]*University of California, Berkeley, California 94720, USA*
[3]*Fermi National Accelerator Laboratory, Batavia, Illinois 60510, USA*
[4]*University of Guanajuato, 3700 Leon, Mexico*
[5]*Illinois Institute of Technology, Chicago, Illinois 60616, USA*
[6]*University of Lausanne, CH-1015 Lausanne, Switzerland*
[7]*Lawrence Berkeley National Laboratory, Berkeley, California 94720, USA*
[8]*University of Michigan, Ann Arbor, Michigan 48109, USA*
[9]*University of South Alabama, Mobile, Alabama, 36688, USA*
[10]*University of Virginia, Charlottesville, Virginia 22904, USA*
(Received 29 November 2004; published 18 March 2005)

A sensitive search for the rare decays $\Omega^- \to \Lambda \pi^-$ and $\Xi^0 \to p\pi^-$ has been performed using data from the 1997 run of the HyperCP (Fermilab E871) experiment. Limits on other such processes do not exclude the possibility of observable rates for $|\Delta S| = 2$ nonleptonic hyperon decays, provided the decays occur through parity-odd operators. We obtain the branching-fraction limits $\mathcal{B}(\Omega^- \to \Lambda \pi^-) < 2.9 \times 10^{-6}$ and $\mathcal{B}(\Xi^0 \to p\pi^-) < 8.2 \times 10^{-6}$, both at 90% confidence level.

The standard model allows $|\Delta S| = 2$ transitions through second-order weak interactions. This approach successfully describes $K^0\overline{K}^0$ mixing, which is currently the only observed $|\Delta S| = 2$ transition. While other $|\Delta S| = 2$ processes have generally been considered too highly suppressed to be observed experimentally, it has been noted that the rate of $K^0\overline{K}^0$ mixing does not exclude nonleptonic $|\Delta S| = 2$ hyperon decays at observable rates, provided that they proceed through new parity-odd channels [1,2]. Measurements can thus be used to set limits on parity-odd contributions to hyperon decays. It is of interest, therefore, to perform sensitive searches for such decays. There is also interest in searches for direct $|\Delta S| = 2$ transitions in B-meson decays [3].

Observation of $|\Delta S| = 2$ nonleptonic hyperon decays at current levels of sensitivity would strongly suggest new physics. He and Valencia [2] have parametrized the strength of any new parity-odd interaction as a ratio to the strength of the electroweak interaction. This ratio is constrained by hyperon branching ratios [2], e.g.,

$$\mathcal{B}(\Xi^0 \to p\pi^-) = 0.9\left(\frac{\alpha_{\text{new}}}{\alpha_{\text{EW}}}\right)^2, \qquad (1)$$

where α_{new} (α_{EW}) is the strength of the new (electroweak) interaction. Current experimental limits on $|\Delta S| = 2$ decays [4] include $\mathcal{B}(\Omega^- \to \Lambda \pi^-) \leq 1.9 \times 10^{-4}$ [5] and

$\mathcal{B}(\Xi^0 \to p\pi^-) \leq 3.6 \times 10^{-5}$ [6], both at 90% confidence level (C.L.). We report a search for these decays using data from the 1997 run of HyperCP (Fermilab Experiment 871). These data are well suited for such studies as they contain large numbers of charged hyperon decays, $\sim 10^9$ $\Xi^- \to \Lambda \pi^-$ and $\sim 10^7$ $\Omega^- \to \Lambda K^-$ decays.

The HyperCP spectrometer is shown schematically in Fig. 1. The spectrometer (described in detail elsewhere [7]) was designed to have large acceptance for the decay chain $\Xi^- \to \Lambda \pi^-$, $\Lambda \to p\pi^-$. In brief, a negatively
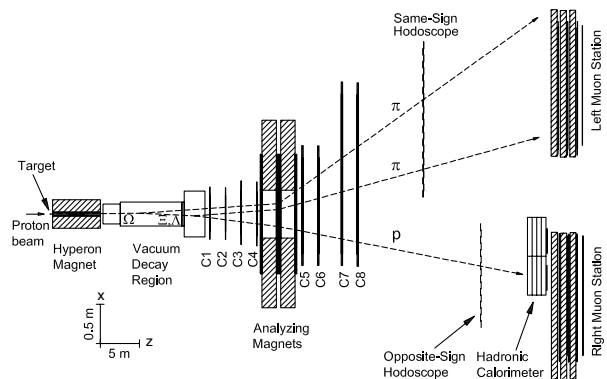

FIG. 1. Plan view of the HyperCP spectrometer. Note that the z scale is compressed by a factor of 10 with respect to the x scale.

charged secondary beam was formed by the interaction of 800 GeV/c primary protons from the Tevatron in a $0.2 \times 0.2 \times 6$ cm^3 copper target, with the secondaries sign and momentum selected by means of a 6.096-m-long curved collimator within a 1.667 T dipole magnetic field (hyperon magnet). The mean secondary momentum was about 160 GeV/c with momenta ranging from 120 to 250 GeV/c. Hyperon decays occurring within a 13-m-long evacuated decay pipe were reconstructed in three dimensions using a series of high-rate, narrow-gap multiwire proportional chambers arrayed on either side of a pair of dipole magnets (analyzing magnets).

The trigger for the data acquisition system [8] used scintillation-counter hodoscopes located sufficiently far downstream of the analyzing magnets so that the hyperon decay products were well separated from the secondary beam. A coincidence was required of at least one ("same-sign") hodoscope hit consistent with a charged particle of the same sign as the secondary beam and at least one "opposite-sign" hit. To suppress muon and low-energy backgrounds the trigger also required a minimum energy deposit in the hadronic calorimeter.

We searched for events consistent with either $\Delta S = 2$ decay chain, $\Omega^- \to \Lambda \pi^-, \Lambda \to p\pi^-$ or $\Omega^- \to \Xi^0 \pi^-$, $\Xi^0 \to p\pi^-$. Also studied were the copious events from the $\Omega^- \to \Lambda K^-, \Lambda \to p\pi^-$ decay sequence used for normalization. Such events all have the topology shown in Fig. 2, with three charged tracks forming two separated vertices. A least-squares geometric fit determined the positions of the primary and secondary vertices, as well as the chi-square (χ^2) value for the event to have the required topology. The reconstructed Ω^- trajectory was traced back through the hyperon magnet using the measured magnetic field to determine its x and y coordinates at the midpoint of the target. Figure 3 compares the $p\pi^-\pi^-$ invariant-mass distribution of all events before event-selection with that of Monte Carlo-generated $\Omega^- \to \Lambda \pi^-, \Lambda \to p\pi^-$ events.

Selection criteria for signal events were based on Monte Carlo simulations and studies of a purified sample of $\Omega^- \to \Lambda K^-, \Lambda \to p\pi^-$ events. Events were required to have three charged tracks with two tracks on the same-sign side of the spectrometer and one on the opposite-sign side. Most $K^- \to \pi^-\pi^-\pi^+$ events were excluded by requiring the invariant mass (treating all three charged tracks as pions) to exceed 0.500 GeV/c^2, 3 standard deviations (σ) above the K^- mass [4]. Since many background events
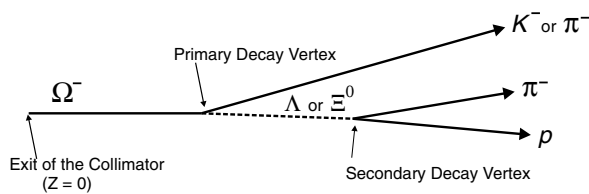
originated from secondary interactions near the exit of the collimator or at the exit windows of the vacuum decay region, all events were required to have a primary-vertex z position between 150 and 1180 cm from the exit of the collimator, well within the vacuum decay region. The secondary vertex was required to be downstream of the primary vertex. The χ^2/degree of freedom from the geometric fit was required to be less than 1.7; this requirement was 98% efficient for $\Omega^- \to \Lambda K^-, \Lambda \to p\pi^-$ events. Selection criteria for the projected Ω^- position at the target were determined using the purified $\Omega^- \to \Lambda K^-, \Lambda \to p\pi^-$ sample. Because of differing resolutions in x and y at the target, an elliptical target cut was used which was 92% efficient for $\Omega^- \to \Lambda K^-, \Lambda \to p\pi^-$.

Additional selection criteria were specific to each mode. For the $\Omega^- \to \Lambda \pi^-, \Lambda \to p\pi^-$ search we required the invariant mass of the $p\pi$ combination forming the secondary vertex to be within ± 2.0 MeV/c^2 (± 1.5 times the rms mass resolution) of the Λ mass [4]. Decay polar angles in the respective hyperon rest frames were calculated with respect to the parent's laboratory frame momentum vector. Background events tended to have a small decay polar angle for the pion in the $\Lambda \pi^-$ center-of-mass system ($\theta_\pi < 0.82$ rad), thus we required $\theta_\pi > 0.82$ rad. The invariant-mass distribution, assuming a $p\pi^-\pi^-$ final state, after all selection cuts is shown in Fig. 4(a). No events were observed within $\pm 9\sigma$ of the expected mass.

For the $\Omega^- \to \Xi^0 \pi^-, \Xi^0 \to p\pi^-$ search, we required that the proton momentum be more than 38% of the $p\pi^-\pi^-$ total momentum, that the invariant mass of the
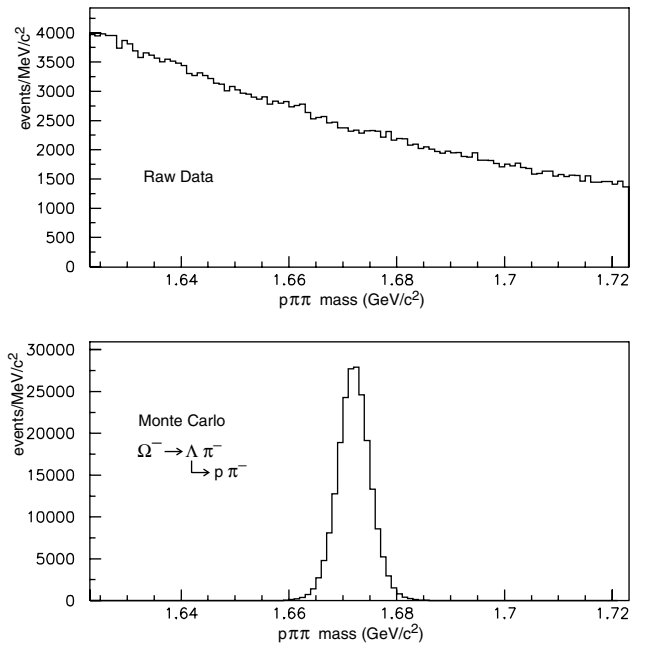

FIG. 3. The $p\pi^-\pi^-$ invariant-mass distribution prior to event selection (top) and from a Monte Carlo simulation of the $\Omega^- \to \Lambda \pi^-, \Lambda \to p\pi^-$ process (bottom).
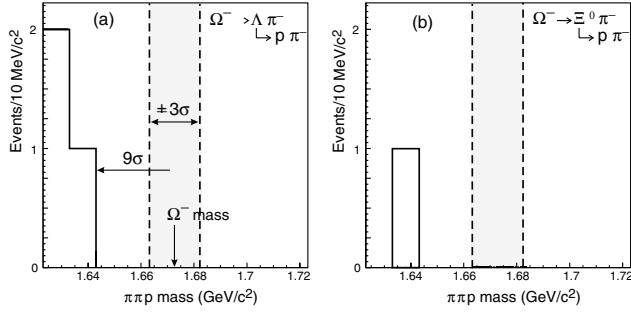

FIG. 2. Event topology for all decays considered here.

FIG. 4. The $p\pi^-\pi^-$ invariant-mass distributions for events satisfying all selection criteria for (a) $\Omega^- \to \Lambda\pi^-$, $\Lambda \to p\pi^-$ and (b) $\Omega^- \to \Xi^0\pi^-$, $\Xi^0 \to p\pi^-$.

TABLE I. Relative spectrometer acceptances vs α decay parameters.

| $\Omega^- \to \Lambda\pi^-; \Lambda \to p\pi^-$ | | | $\Omega^- \to \Xi^0\pi^-; \Xi^0 \to p\pi^-$ | | |
α_{Ω^-}	α_Λ	Rel. Acc.	α_{Ω^-}	α_{Ξ^0}	Rel. Acc.
-1.00	0.642	1.17	-0.05	-1.0	1.05
-0.75	0.642	1.13	-0.05	0.0	1.05
-0.50	0.642	1.09	-0.05	1.0	1.04
-0.25	0.642	1.05	0.09	-1.0	0.98
0.00	0.642	1.00	0.09	0.0	1.00
0.25	0.642	0.94	0.09	1.0	1.02
0.50	0.642	0.87	0.23	-1.0	0.92
0.75	0.642	0.79	0.23	0.0	0.95
1.00	0.642	0.70	0.23	1.0	0.98

$p\pi$ combination forming the secondary vertex be within ± 5.0 MeV/c^2 ($\pm 3.0\sigma$) of the Ξ^0 mass [4], that the z position of the daughter-hyperon decay vertex be within the vacuum decay region, and that the polar angle of the proton in the $p\pi$ center-of-mass frame be less than 2.97 rad. The $p\pi^-\pi^-$ invariant-mass distribution for events satisfying all selection criteria is shown in Fig. 4(b). Again, no events were observed within $\pm 9\sigma$ of the expected mass.

The spectrometer acceptances for these decays were estimated using a Monte Carlo simulation. The generated Ω^- momentum and position distributions at the target were tuned to match those observed in the data for a purified sample of $\Omega^- \to \Lambda K^-$, $\Lambda \to p\pi^-$ decays. For all decay modes, the acceptance includes the probability that the parent decay occur within the vacuum decay region. The geometric acceptance of the spectrometer was determined primarily by the apertures of the analyzing magnets. Because of the larger Q values for $\Omega^- \to \Lambda\pi^-$ and $\Xi^0 \to p\pi^-$ compared to those of $\Omega^- \to \Lambda K^-$ and $\Lambda \to p\pi^-$, tracks from signal-mode decays would be approximately 3 times more likely to miss the magnet apertures and be lost. For events accepted in the magnet apertures, the trigger efficiency ranged from 93% for $\Omega^- \to \Lambda\pi^-$, $\Lambda \to p\pi^-$ candidates to 99% for $\Omega^- \to \Lambda K^-$, $\Lambda \to p\pi^-$ events. The candidate signal- and normalizing-mode events were all accepted by the same trigger, so it was not necessary to cross calibrate trigger efficiencies by mode. Offline event-selection efficiencies differed considerably by mode, since restrictive selection criteria to suppress background were required for the signal modes but not for the normalizing mode. To study the systematic uncertainties of the selection efficiencies, the selection criteria were varied. This produced only slight changes in the results.

The α decay parameter for $\Omega^- \to \Lambda K^-$ has recently been precisely measured and found to be small, but may not be zero [9], while the measured value for $\Omega^- \to \Xi^0\pi^-$ is less precise and is consistent with zero [4]. Theory predicts little parity violation in the dominant Ω^- decays [10] (as observed); however, we cannot exclude large

decay asymmetries for $\Omega^- \to \Lambda\pi^-$. Similarly, we do not know the size of parity violation in $\Xi^0 \to p\pi^-$. We therefore assign zero to the value of α for $\Omega^- \to \Lambda\pi^-$ and $\Xi^0 \to p\pi^-$. The dependence of the acceptance on α is tabulated in Table I. The acceptance times the selection efficiency (including the maximal acceptance variation due to uncertainty in α) was $6.2^{+0.9}_{-1.0}\%$ for $\Omega^- \to \Xi^0\pi^-$, $\Xi^0 \to p\pi^-$, $6.9^{+1.8}_{-2.2}\%$ for $\Omega^- \to \Lambda\pi^-$, $\Lambda \to p\pi^-$, and $(34.9 \pm 1.2)\%$ for $\Omega^- \to \Lambda K^-$, $\Lambda \to p\pi^-$.

Signal-mode branching ratios were normalized using the observed $\Omega^- \to \Lambda K^-$, $\Lambda \to p\pi^-$ sample, whose invariant-mass distribution is shown in Fig. 5. The figure includes a fit of the mass distribution to a Gaussian plus a second-order polynomial. The number of normalizing-mode decays was estimated using three different background-subtraction methods. In all three, an estimate of the background was subtracted from the total number of events observed within $\pm 3\sigma$ of the Ω mass. The first background estimate was the sum of all events within $\pm 3\sigma$ of the Ω mass minus the integral of the fitted second-order polynomial over that region. In the second
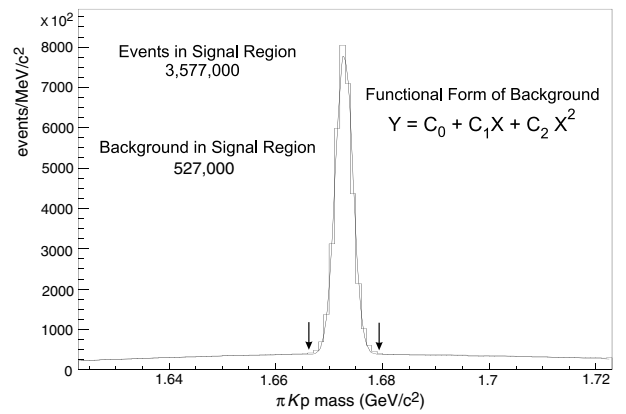

FIG. 5. Observed $pK^-\pi^-$ invariant-mass distribution. The number of events in the $\Omega^- \to \Lambda K^-$, $\Lambda \to p\pi^-$ peak was used to normalize the upper limits presented here. The arrows indicate $\pm 3\sigma$ in mass resolution.

method, a fit was performed over a limited region ($\pm 3\sigma$) around the Ω mass to a Gaussian plus a constant. The third method averaged the two bins at $\pm 3\sigma$ and multiplied this by the number of bins within the $\pm 3\sigma$ window. All methods gave similar results. The final estimate of the number of observed normalizing events was taken as the average of the three estimates, $(3.050 \pm 0.023) \times 10^6$, with the uncertainty defined as half the difference between the largest and smallest estimates (corresponding to about 1σ, assuming Gaussian statistics). After correcting for acceptance and selection efficiencies, and accounting for the measured branching fractions, the total number of Ω^- baryons exiting the collimator was $(20.2 \pm 0.8) \times 10^6$.

Signal-mode branching fractions were obtained from

$$\mathcal{B}(\Omega^- \to \Lambda \pi^-) = \frac{N_{\text{sig}}}{N_{\text{norm}}} \frac{A_{\text{norm}}}{A_{\text{sig}}} \mathcal{B}(\Omega^- \to \Lambda K^-), \quad (2)$$

$$\mathcal{B}(\Xi^0 \to p\pi^-) = \frac{N_{\text{sig}}}{N_{\text{norm}}} \frac{A_{\text{norm}}}{A_{\text{sig}}}$$
$$\times \frac{\mathcal{B}(\Omega^- \to \Lambda K^-)\mathcal{B}(\Lambda \to p\pi^-)}{\mathcal{B}(\Omega^- \to \Xi^0 \pi^-)}. \quad (3)$$

Here N denotes the number of events observed and A the acceptance for a given mode, with subscripts sig designating the signal mode in question and norm the normalizing mode $\Omega^- \to \Lambda K^-, \Lambda \to p\pi^-$. The number of signal events observed is zero in each case. The measured branching ratios entering into Eqs. (2) and (3) are $\mathcal{B}(\Omega^- \to \Lambda K^-) = (67.8 \pm 0.7)\%$, $\mathcal{B}(\Lambda \to p\pi^-) = (63.9 \pm 0.5)\%$, and $\mathcal{B}(\Omega^- \to \Xi^0 \pi^-) = (23.6 \pm 0.7)\%$ [4]. Systematic uncertainties include the uncertainties of these branching ratios, that of the normalizing mode background subtraction, and, most importantly, those associated with acceptances and event selection.

To derive 90% C.L. upper limits for the numbers of events observed (U_n), we included systematic uncertainties [11] as follows:

$$U_n = U_{n0}[1 + (U_{n0} - n)\sigma_r^2/2]. \quad (4)$$

Here U_{n0} represents the statistical limit based on the Poisson distribution with no systematic uncertainties, n is the number of observed events, and σ_r is the relative systematic uncertainty. In our case ($n = 0$), Eq. (4) reduces to

$$U_0 = 2.3(1 + 2.3\sigma_r^2/2). \quad (5)$$

The relative uncertainty (including uncertainties in the acceptance, selection, normalization, and branching ratios) was 16% for $\Omega^- \to \Xi^0 \pi^-, \Xi^0 \to p\pi^-$ and 32% for $\Omega^- \to \Lambda \pi^-, \Lambda \to p\pi^-$. Upper limits on the numbers of observed events at the 90% C.L. thus determined are 2.4 events for $\Xi^0 \to p\pi^-$ and 2.6 for $\Omega^- \to \Lambda \pi^-$, comparable to the 2.3 events obtained from a frequentist statistical treatment of the Poisson fluctuation alone [4]. We thus obtain $\mathcal{B}(\Omega^- \to \Lambda \pi^-) < 2.9 \times 10^{-6}$ and $\mathcal{B}(\Xi^0 \to p\pi^-) < 8.2 \times 10^{-6}$, both at 90% C.L. These results represent improvements by 1 to 2 orders of magnitude over previous measurements.

*Corresponding author.
  Electronic address: whitec@iit.edu

[1] S. Glashow, Phys. Rev. Lett. **6**, 196 (1961).
[2] X. G. He and G. Valencia, Phys. Lett. B **409**, 469 (1997); **418**, 443(E) (1998).
[3] S. Fajfer and P. Singer, Phys. Rev. D **62**, 117702 (2000); S. Fajfer and P. Singer, Phys. Rev. D **65**, 017301 (2002).
[4] Particle Data Group, S. Eidelman *et al.*, Phys. Lett. B **592**, 1 (2004).
[5] M. Bourquin *et al.*, Nucl. Phys. **B241**, 1 (1984).
[6] C. Geweniger *et al.*, Phys. Lett. **57B**, 193 (1975).
[7] R. A. Burnstein *et al.*, hep-ex/0405034.
[8] Y. C. Chen *et al.*, Nucl. Instrum. Methods Phys. Res., Sect. A **455**, 424 (2000).
[9] Y. C. Chen *et al.*, Phys. Rev. D **71**, 051102(R) (2005).
[10] M. Suzuki, Prog. Theor. Phys. **32**, 138 (1964); Y. Hara, Phys. Rev. **150**, 1175 (1966); J. Finjord, Phys. Lett. **76B**, 116 (1978).
[11] R. D. Cousins and V. L. Highland, Nucl. Instrum. Methods Phys. Res., Sect. A **320**, 331 (1992).